Metabolic profiles of whole serum and serum-derived exosomes are different in head and neck cancer patients treated by radiotherapy

Anna Wojakowska
Institute of Bioorganic Chemistry Polish Academy of Sciences
Aneta Zebrowska
Maria Sklodowska-Curie National Research Institute of Oncology, Gliwice Branch
Agata Skowronek
Maria Sklodowska-Curie National Research Institute of Oncology, Gliwice Branch
Tomasz Rutkowski
Maria Sklodowska-Curie National Research Institute of Oncology, Gliwice Branch
Krzysztof Polański
Wellcome Sanger Institute
Piotr Widlak
Maria Sklodowska-Curie National Research Institute of Oncology, Gliwice Branch
Monika Pietrowska
Maria Sklodowska-Curie National Research Institute of Oncology, Gliwice Branch
Lukasz Marczak (lukasmar@ibch.poznan.pl)
Institute of Bioorganic Chemistry Polish Academy of Sciences https://orcid.org/0000-0001-8602-0077

Research

Keywords: head and neck cancer, exosomes, serum, radiotherapy, metabolomics, GC/MS

Posted Date: July 21st, 2020

DOI: https://doi.org/10.21203/rs.3.rs-44974/v1

Version of Record: A version of this preprint was published at Journal of Personalized Medicine on November 13th, 2020. See the published version at https://doi.org/10.3390/jpm10040229.

Abstract

Background

Serum metabolome reflects a general patient's body response to both disease state (e.g., cancer) and implemented treatment (e.g., radiotherapy, RT). Though serum-derived exosomes are an emerging type of liquid biopsy, a metabolite content of these vesicles remains under-researched yet. In this pilot study, we aimed to compare metabolite profiles of the whole serum and serum-derived exosomes in the context of differences between cancer patients and healthy controls as well as patients' response to RT.

Methods

Serum samples were collected from 10 healthy volunteers and 10 patients with head and neck cancer, in the latter group samples were taken before and after the end of RT. Exosomes were isolated from serum by the size-exclusion chromatography. Metabolites were purified from the complete serum and exosomes using a methanol extraction and analyzed by the gas chromatography-mass spectrometry (GC-MS).

Results

An untargeted GC-MS-based approach allowed the detection of 182 and 46 metabolites in serum and exosomes, respectively (33 compounds were present in both types of specimens). The unsupervised analyses revealed that metabolite profiles of the whole serum but not serum-derived exosomes enabled the separation of all 3 groups of samples. There were 27 compounds whose serum levels were markedly different (large effect size) between control and cancer samples and 12 compounds whose serum levels were markedly different between cancer pre-RT and post-RT samples. On the other hand, only 4 metabolites present in exosomes showed markedly different levels between cancer and control samples. Noteworthy, metabolites that differentiated cancer and control samples, either serum or exosomes, were associated with energy metabolism pathways. Serum metabolites affected by RT were associated with pathways involved in the metabolism of amino acids, sugars, lipids, and nucleotides.

Conclusions

Metabolite profile of serum-derived exosomes is less complex than that of the complete serum. However, cancer-specific features of energy metabolism could be detected in both types of specimens. On the other hand, in contrast to RT-induced changes observed in serum metabolome, this pilot study did not reveal a specific radiation-related pattern of exosome metabolites.

Introduction

Head and neck cancer (HNC) is the sixth most common malignancy worldwide. The incidence of HNC exceeds half a million annually and accounts for approximately 6% of all cancer cases worldwide [1, 2]. Although over the last decade we observe improvement in the treatment of HNC, there is still a need for new biomarkers of this cancer because, despite molecular heterogeneity of HNC, tumor location and classical staging remain the major criteria of the treatment selection [3]. Radiotherapy (RT), used either alone or in combination with other treatment modalities (surgery, chemotherapy, or immunotherapy) is the major modality in the HNC treatment. The major benefit of RT is well established local control of the tumor. However, ionizing radiation induces damage to the adjacent healthy tissues, which is reflected at the systemic level in body fluids [4–7]. Hence, detection in the patient's blood of molecular fingerprint of the body response to the treatment, which could potentially enable monitoring and prediction of radiation toxicity, is another important aspect of HNC diagnostics.

Various types of "omics" studies (genomics, transcriptomics, proteomics, metabolomics) using different sources of samples (blood, urine, saliva, tissues) uncovered molecules and genes of potential use as clinical biomarkers [8, 9]. Cancer cells' metabolism differs from one of the healthy cells and it's considered as the closest footprint of cancer phenotype. This is why metabolomics studies are one of the fastest-growing areas of cancer researches in the last decades. Recent studies revealed disparities in the metabolite profile between diseased and normal states as well as between miscellaneous types of cancer or various stages of the disease. Therefore, altered metabolic pathways in various cancer systems might be used to identify biomarkers in terms of diagnosis, prognosis, or treatment schedule choice [10, 11]. NMR-based metabolomics study revealed an increased level of glucose, ketone bodies, ornithine, asparagine, and 2-hydroxybutyrate while decreased levels of citric acid cycle (TCA cycle) intermediates (citrate, succinate, and formate), lactate, alanine, and other gluconeogenic amino acids in sera of patients with HNC [12]. Another GC/MS-based metabolomics analysis of serum and tissues of HNC patients revealed different metabolite profiles in patients with different treatment outcomes. In patients with disease relapse serum levels of metabolites related to the glycolytic pathway (especially glucose, ribose, fructose) were higher while serum levels of amino acids (lysine and trans-4-hydroxy-L-proline) were lower than in samples of patients without disease relapse [13]. Hence, one could conclude that the altered energy metabolism (mostly the switch from the TCA cycle to glycolysis and fatty acid oxidation), apparently associated with the Warburg effect, is characteristic for patients with HNC [12–15]. Moreover, a few studies addressed therapy-induced changes in metabolic profiles of HNC, that revealed compounds which levels were associated with the treatment escalation (e.g. radiation dose during radiotherapy) or the intensity of treatment toxicity [16–18]. However, the knowledge about molecular mechanisms involved in radiation-induced changes of the patient's metabolome remains rather limited.

In the present study, the GC/MS approach was applied for profiling serum metabolites of HNC patients who underwent RT to uncover metabolome changes induced by radiation. Furthermore, we included in the study another emerging biospecimen – exosomes circulating in patients' blood. Exosomes are virus-sized (50–150 nm) vesicles of endosomal origin released by the majority of cell types, either normal and cancerous [19]. Exosomes and other classes of extracellular vesicles (EVs) play an essential role in cancer biology being the key mediators of communication between cells [20, 21]. EVs present in the blood

and other biofluids represent an interesting type of so-called liquid biopsy, which is an emerging source of potential biomarkers [22, 23]. There is growing evidence for the increased level of EVs in biofluids of cancer patients as well as radiation-induced enhancement of exosome secretion [24, 25]. However, though literature data support the important role of transcriptome and proteome content of cancer-related EVs, much less is known about their metabolome component [20]. Similarly, the data regarding radiation-induced changes in the EVs cargo refer mainly to its transcriptome and proteome [26, 27]. Hence, searching for RT-related changes in the serum metabolome of HNC patients, we also aimed to address metabolite profiles of serum-derived EVs.

Materials And Methods

Samples collection. Ten patients with squamous cell carcinoma located in pharynx regions (6 males and 4 females, aged between 49 and 71 years) treated by the continuous accelerated irradiation (CAIR) scheme with a daily fraction dose of 1.8 Gy to the total dose 64–72 Gy were included in the study. Blood samples were collected before RT (cancer pre-treatment sample A) and one month after the end of RT (cancer post-treatment sample B). Moreover, ten healthy volunteers constituted age- and sex-matched control group (control sample C). The study was approved by the appropriate local Ethics Committee (NRIO; approval no. 1/2016) and all participants provided informed consent indicating their conscious and voluntary participation. Five mL of blood was collected into an anticoagulant-free tube (Becton Dickinson, Franklin Lakes, NJ, USA; 367955), incubated for 30 min at 20 °C then centrifuged at 1,000xg for 10 min at 4 °C. The serum (supernatant) was transferred to clean tubes stored at -80 °C until analyzed.

Exosomes isolation and characterization. The method for isolation of exosomes from small amounts of serum was established and optimized in our laboratory as described previously [28]. Briefly, exosomes were isolated from serum (500 µl) by differential centrifugation (1,000 x g and 10,000 x g for 10 and 30 min. respectively, at 4 °C) and filtration through 0.22 µm filter followed by the size exclusion chromatography (SEC). SEC was performed using hand-packed columns (BioRad) filled with 10 ml of Sepharose CL-2B (GE Healthcare), conditioned previously with phosphate buffer saline (PBS). Consecutive fractions (500 µl each) were collected and characterized for EV enrichment (fraction #8 was used for further analyses). The size of vesicles in the SEC fractions was evaluated by the dynamic light scattering (DLS) using Zetasizer Nano-ZS90 instrument (Malvern Instruments, Malvern, UK) and by transmission electron microscopy. Exosome markers CD63 and CD81 were analyzed by Western blots as reported in detail elsewhere [28]. The concentration of proteins in the analyzed samples was assessed using the PierceTM BCA Protein Assay kit (Thermo Fisher Scientific, Waltham, MA, USA; 23225) according to the manufacturer's instructions.

Metabolite extraction. 200 µl of 80% MeOH was added to 25 µl of serum sample. In the case of exosomes, 2 ml of 100% MeOH was added to 500 µl of the selected SEC fraction. The mixture was vortexed and centrifuged for 5 min then sonicated for 10 min. The mixture was placed at -20 °C for 20 min. and after that centrifuged for 10 min. at 23,000 x g at 4 °C. The supernatant was transferred to a

new tube and evaporated in a SpeedVac concentrator (CentriVap Concentrator, Labconco, USA). The dried extract was then derivatized with 25 µl of methoxyamine hydrochloride in pyridine (20 mg/ml) at 37 °C for 90 min. with agitation. The second step of derivatization was performed by adding 40 µl of MSTFA and incubation at 37 °C for 30 min with agitation. Samples were subjected to GC/MS analysis directly after derivatization.

GC-MS analysis. The GS/MS analysis was performed using TRACE 1310 gas chromatograph connected with TSQ8000 triple-quad mass spectrometer (Thermo Scientific, USA). A DB-5MS bonded-phase fused-silica capillary column (30 m length, 0.25 mm inner diameter, 0.25 µm film thickness) (J&W Scientific Co., USA) was used for separation. The GC oven temperature gradient was as follows: 70 °C for 2 min, followed by 10 °C/min up to 300 °C (10 min), 2 min at 70 °C, raised by 8 °C/min to 300 °C and held for 16 min at 300 °C. For sample injection, PTV injector was used in a range of 60 to 250 °C, transfer line temp. was set to 250 °C, source to 250 °C. Spectra were recorded in m/z range of 50–850 in EI + mode with an electron energy of 70 eV. Raw MS-data were converted to abf format and analyzed using MSDial software package v. 3.96. To eliminate retention time (Rt) shift and to determine the retention indexes (RI) for each compound, the alkane series mixture (C-10 to C-36) was injected into the GC/MS system. Identified artifacts (alkanes, column bleed, plasticizers, MSTFA, and reagents) were excluded from further analyses. Obtained normalized (using total ion current (TIC) approach) results were then exported to Excel for pre-formatting and then tables were used for statistical analyses.

Statistical and chemometric analyses. Differences between independent samples were assessed using the T-test, Welch test, or U-Mann-Whitney test, dependent on the normality and homoscedasticity of data (assessed via the Shapiro-Wilk test and Levene test respectively). For paired samples, the paired t-test or Wilcoxon test were used based on the normality of the difference distribution. In each case, the Benjamini-Hochberg protocol was used for the false discovery rate (FDR) correction. However, due to the small sample size, none of the differences remained significant after the FDR correction. Hence, the effect size analysis was employed to overcome this problem [29]. For independent samples, the rank-biserial coefficient of correlation (RBCC; an effect size equivalent of the U-Mann-Whitney test) was applied; the effect size ≥ 0.3 and ≥ 0.5 was considered medium and high, respectively [30]. For paired samples, the paired t-test derived Cohen's d effect size was applied; the effect size ≥ 0.5 and ≥ 0.8 was considered medium and high, respectively [31] (Rosenthal, 1994). Principal Component Analysis (PCA) and Hierarchical Cluster Analysis (HCA) based on the Euclidean distance method were performed to illustrate general similarities between samples. Metabolic pathways were associated with differentiating compounds that showed high and medium effect size using the quantitative enrichment analysis on the MetaboAnalyst platform (https://www.metaboanalyst.ca/MetaboAnalyst/ModuleView.xhtml). Obtained enriched pathways and their connections together with statistical information were further analyzed in Cytoscape. The DyNet addon was used to compare two networks and find interacting nodes [32]; fold enrichment and significance of enrichment (FDR) were coded by size and color of nodes, respectively.

Results

Extracellular vesicles isolated from serum by size exclusion chromatography were characterized by their size and the presence of specific biomarkers. The SEC fraction #8 was enriched in vesicles, which size was estimated in a range between 50 and 150 nm by the DLS measurement (with the maximum at 100-120 nm) (**Figure 1A**). The size of the isolated vesicles was confirmed by transmission electron microscopy (TEM) (**Figure 1B**). Furthermore, the presence of exosome biomarkers, tetraspanins CD63 and CD81, was confirmed in the same fraction by Western blot analysis (the same proteins remained undetected in the whole serum) (**Figure 1C**). Considering their specific size and the presence of exosome-specific biomarkers, vesicles present in the analyzed fraction were called exosomes for simplicity, yet other subpopulations of the small EVs could be also present in this material.

The GC-MS-based approach was used for profiling of metabolites in the whole serum and the corresponding serum-derived exosomes of HNC patients, in either pre-treatment (A) and post-treatment (B) samples, or samples of matched healthy controls (C). In general, the untargeted approach allowed the identification of 182 metabolites in serum samples and 46 metabolites in exosome samples, of which 33 metabolites overlapped; the complete list of 195 identified compounds is presented in **Supplementary Table S1**. **Figure 2** illustrates the distribution of different classes of small metabolites identified by GC-MS in serum and serum-derived exosome samples. Among the most numerous classes of metabolites common for serum and exosomes were fatty acids, sugar alcohols, and carboxylic acids (22%, 15%, and 12% of all identified compounds, respectively). Noteworthy, amino acids that were the most numerous group of metabolites in serum samples were markedly less frequent in exosome samples (21% vs. 7% of all identified compounds, respectively, which corresponded to 40 and 3 compounds). All identified metabolites were used to perform unsupervised clustering of samples. The metabolite composition of the whole serum enabled the relatively good separation of all three groups of samples using either the principal component analysis (**Figure 3A**) and the hierarchical cluster analysis (**Figure 4A**). Noteworthy, control samples C were more similar to cancer pre-treatment samples A than to cancer post-treatment samples B, which indicated the additional putative treatment-related differential component. In contrast, neither the PCA nor the HCA type of analysis allowed the separation of corresponding groups when samples of serum-derived exosomes were analyzed (**Figure 3B** and **Figure 4B**).

In the next step, specific metabolites were detected whose abundances were significantly different between groups. First, we looked for compounds that differentiated cancer patients (pre-treatment samples A) from healthy individuals (control samples C). There were 27 compounds whose serum levels were markedly different (large effect size) between control and cancer samples. These included 12 metabolites upregulated (4 amino acids, 4 fatty acids, 2 purines, 1 glycerolipid, and lactose) and 15 metabolites downregulated (3 carboxylic acids, 3 purines, 3 sugars, 2 fatty acids, serotonin, acetyl-hexosamine, isoleucine, and phosphate) in cancer samples, which were listed in **Table 1**. Furthermore, there were 18 cancer-upregulated and 38 cancer-downregulated compounds where differences showed a medium effect size (**Supplementary Table S1**). On the other hand, there were only a few compounds whose abundance was significantly different in serum-derived exosomes from healthy controls and cancer patients. 1-Hexadecanol was markedly upregulated while citric acid, 4-hydroxybenzoic acid, and propylene glycol were markedly downregulated (large effect size) in exosomes from cancer patients

(**Table 1**). Moreover, there were 7 metabolites where differences showed medium effect size, including myo-inositol, linoleic acid, succinic acid, and glyceric acid downregulated in cancer samples (**Supplementary Table S1**). Furthermore, metabolites whose levels were different between control and cancer samples (either large effect size or medium effect size) were annotated with their corresponding metabolic pathways. We observed that overrepresented pathways associated with metabolites discriminating cancer patients and healthy controls in both whole serum and serum-derived exosome samples included ones involved in energy production (citric acid cycle, Warburg effect, pyruvate metabolism, mitochondrial electron transport chain) and inositol metabolism. Pathways associated specifically with serum metabolites included metabolism of amino acids, sugars, and lipids. On the other hand, pathways associated with metabolites specific for serum-derived exosomes included oxidation of fatty acids and ketone body metabolism (**Figure 5A**).

In the second step, we looked for metabolites whose abundance was different in serum and serum-derived exosomes of cancer patients between pre-treatment samples A and post-treatment samples B, which allowed detection of changes related to RT. There were 12 compounds whose serum levels were markedly different (large effect size) between pre-treatment and post-treatment cancer samples. These included 4 metabolites upregulated (including hypotaurine and serotonin) and 8 metabolites downregulated in post-RT serum samples, which are listed in **Table 2**. Furthermore, there were 29 RT-upregulated and 12 RT-downregulated compounds where differences showed a medium effect size (**Supplementary Table S1**). In marked contrast, only two metabolites detected in serum-derived exosomes (glycerol and cholesterol) showed reduced levels (medium effect size) in post-RT samples. Finally, metabolites whose abundance was different in pre-RT and post-RT samples (either large effect size or medium effect size) were annotated with their corresponding metabolic pathways. Over-represented pathways associated with metabolites whose serum levels were affected by RT included those involved in the metabolism of different classes of compounds (amino acids, sugars, nucleotides, lipids, and biogenic amines), which indicated multifaceted effects of radiation on serum metabolome profile (**Figure 5B**).

Discussion

Serum-derived exosomes, an emerging type of liquid biopsy, are a potential source of biomarkers. However, their metabolite compartment is less characterized compared to proteome or miRNome [20]. Here we compared metabolite profiles of whole human serum and serum-derived exosomes and found significantly fewer compounds in the latter specimen. This difference could be caused both by a lower number of compounds present in vesicles *per se* (i.e., their lower complexity) or their lower concentration, which hindered their detection by the method used in our approach. Hence, a direct comparison of metabolic pathways associated with compounds present in whole serum and serum-derived vesicles could be compromised by this discrepancy. Nevertheless, it has to be emphasized that the major metabolic hallmark of cancer – the modified energy metabolism could be detected in both specimens. In head and neck cancer, as in many other types of cancers, tumor cells can alter their energy metabolism by switching from the citric acid cycle (TCA cycle) to glycolysis and oxidation of fatty acids as a backup

mechanism for energy production [16], which phenomenon is known as the Warburg effect [33]. Our study confirmed that metabolites associated with processes involved in energy metabolism, including glycolysis, gluconeogenesis, Warburg effect, TCA cycle, pyruvate metabolism, and mitochondrial electron transport chain showed different levels in samples of HNC patients and healthy controls. Importantly, features associated with this characteristic cancer phenotype were observed in both whole serum and serum-derived exosomes. Noteworthy, pathways associated with metabolites specific for serum-derived exosomes of cancer patients included oxidation of fatty acids and ketone body metabolism. Beta-oxidation of fatty acids and increased lipolysis, which is reflected as the accumulation of ketone bodies, was reported in HNC patients as a potential backup mechanism for energy production [12]. Previous studies reported that molecules involved in fatty acids transport and storage as well as lipolysis and fatty acids oxidation are enriched in EVs and suggested that fatty acid transport from cell-to-cell and across cell membranes could be mediated by EVs [34, 35]. Hence, a specific role of serum EVs in the transmission of mediators associated with cancer-related lipid metabolism deserves further attention.

Our study revealed that RT affected serum levels of several amino acids, biogenic amines, sugars, nucleotides, lipids, and fatty acids, which mirrored potential RT-induced changes in a plethora of metabolic pathways ongoing in a patient's body. It was previously reported that altered metabolism of amino acid plays an important role in the response of HNC patients to RT [36]. For example, Boguszewicz and co-workers [4] demonstrated that decreased serum level of alanine, the main substrate for gluconeogenesis during fasting and cachexia, correlated with the acute radiation toxicity-associated weight loss in HNC patients undergoing RT. The whole-body response to irradiation frequently involves molecules associated with oxidative stress and inflammation [18]. Hence, it is noteworthy that hypotaurine, which is involved in protection against oxidative stress as an effect of RT [37], was significantly elevated in post-RT serum samples. Moreover, RT-induced changes in serum level of phospholipids potentially associated with the inflammatory response and disruption of plasma membranes were previously reported in samples HNC patients [38, 39]. Here we found that compounds associated with lipid metabolism (e.g., phosphatidylethanolamine and phosphatidylcholine biosynthesis) were affected in post-RT serum samples, which confirmed the general RT-related metabolic phenotype. Interestingly, however, very few RT-related changes were detected in the metabolic profile of serum-derived exosomes. This was in contrast to significant radiation-induced changes observed at the level of the proteome [40] and miRNome [41] of exosomes released by HNC cells. Exosomes released by irradiated cells are known mediators of radiation bystander effect and other aspects of radiation-related cell-to-cell signaling [42]. Hence, the potential role of metabolites in exosomes-mediated radiation-related signaling should be addressed in further studies.

Conclusions

In this pilot study, we compared metabolite profiles of the whole serum and serum-derived exosomes of healthy controls and patients treated with RT due to head and neck cancer aimed to revel cancer-specific and/or RT-related features. We found that the metabolite profile of serum-derived exosomes is less complex than that of the complete serum. However, cancer-specific features of energy metabolism were

detected in both types of specimens, which confirmed the feasibility of cancer biomarkers based on exosome metabolites. On the other hand, in contrast to RT-induced changes observed in serum metabolome, this pilot study did not reveal a specific pattern of radiation-related changes in exosome metabolites. Hence, further metabolomics study with a larger cohort of individuals treated with RT is necessary to validate a hypothetical radiation signature of serum exosomes.

Abbreviations

CAIR
Continuous accelerated irradiation
DLS
Dynamic light scattering
EVs
Extracellular vesicles
FDR
False discovery rate
GC-MS
Gas chromatography-mass spectrometry
HCA
Hierarchical Cluster Analysis
HNC
Head and neck cancer
MSTFA
N-Methyl-N-(trimethylsilyl)trifluoroacetamide
PBS
Phosphate buffer saline
PCA
Principal Component Analysis
RBCC
Rank-biserial coefficient of correlation
RI
Retention indexes
RT
Radiotherapy
SEC
Size exclusion chromatography
TCA cycle
Citric acid cycle
TEM
transmission electron microscopy

TIC
Total ion current

Declarations

Ethics approval and consent to participate: The study involving human participants adhered to the tenets of the Declaration of Helsinki and was approved by the Bioethical Committee of the Maria Sklodowska-Curie National Research Institute of Oncology, Poland (decision number DO/DGP/493/4/06/1/2016/G). All participants provided informed consent indicating their conscious and voluntary participation.

Consent for publication: Not applicable.

Availability of data and materials: The datasets used and analyzed during the current study are available from the corresponding author on reasonable request.

Competing interests: The authors declare that they have no competing interests.

Funding: This work was supported by the National Science Centre, Poland, grant no. 2015/17/B/NZ5/01387 (T.R., P.W.), 2016/22/M/NZ5/00667 (A.Z., A.S., M.P.), and 2017/26/D/NZ2/00964 (A.W., LM).

Authors' contributions: A.W. analyzed MS data, interpreted results and prepared the manuscript, A.Z. and A.S. carried out the experiments, T.R. collected and described the clinical material, K.P. performed statistical analyses, P.W. interpreted results and reviewed the final version of the manuscript, L.M. performed MS analysis, analyzed and interpreted MS data, M.P. designed and financed the study. All authors read and approved the final version of the manuscript.

Acknowledgements: Not applicable

References

1. Gupta B, Johnson NW, Kumar N. Global Epidemiology of Head and Neck Cancers: A Continuing Challenge. Oncology (Switzerland). 2016;91:13–23.
2. Budach V, Tinhofer I. Novel prognostic clinical factors and biomarkers for outcome prediction in head and neck cancer: a systematic review. The Lancet Oncology. 2019;20:e313–26.
3. Economopoulou P, de Bree R, Kotsantis I, Psyrri A. Diagnostic tumor markers in head and neck squamous cell carcinoma (HNSCC) in the clinical setting. Frontiers in Oncology. 2019;9 AUG:827. doi:10.3389/fonc.2019.00827.
4. Boguszewicz, Bieleń A, Mrochem-Kwarciak J, Skorupa A, Ciszek M, Heyda A, et al. NMR-based metabolomics in real-time monitoring of treatment induced toxicity and cachexia in head and neck cancer: a method for early detection of high risk patients. Metabolomics. 2019;15.
5. Baskar R, Lee KA, Yeo R, Yeoh KW. Cancer and radiation therapy: Current advances and future directions. International Journal of Medical Sciences. 2012;9:193–9.
6. Darby SC, Cutter DJ, Boerma M, Constine LS, Fajardo LF, Kodama K, et al. Radiation-Related Heart Disease: Current Knowledge and Future Prospects. International Journal of Radiation Oncology Biology Physics. 2010;76:656–65.
7. Travis LB, Ng AK, Allan JM, Pui CH, Kennedy AR, Xu XG, et al. Second malignant neoplasms and cardiovascular disease following radiotherapy. Health Phys. 2014;106:229–46.
8. Pinu FR, Beale DJ, Paten AM, Kouremenos K, Swarup S, Schirra HJ, et al. Systems Biology and Multi-Omics Integration: Viewpoints from the Metabolomics Research Community. Metabolites. 2019;9:76. doi:10.3390/metabo9040076.
9. Wheelock CE, Goss VM, Balgoma D, Nicholas B, Brandsma J, Skipp PJ, et al. Application of 'omics technologies to biomarker discovery in inflammatory lung diseases. European Respiratory Journal. 2013;42:802–25. doi:10.1183/09031936.00078812.
10. Patel S, Ahmed S. Emerging field of metabolomics: Big promise for cancer biomarker identification and drug discovery. Journal of Pharmaceutical and Biomedical Analysis. 2015;107:63–74.
11. Armitage EG, Barbas C. Metabolomics in cancer biomarker discovery: Current trends and future perspectives. Journal of Pharmaceutical and Biomedical Analysis. 2014;87:1–11.
12. Tiziani S, Lopes V, Günther UL. Early stage diagnosis of oral cancer using 1H NMR-Based metabolomics1,2. Neoplasia. 2009;11:269–76.
13. Yonezawa K, Nishiumii S, Kitamoto-Matsuda J, Fujita T, Morimoto K, Yamashita D, et al. Serum and tissue metabolomics of head and neck cancer. Cancer Genomics and Proteomics. 2013;10:233–8.
14. Hsieh YT, Chen YF, Lin SC, Chang KW, Li WC. Targeting cellular metabolism modulates head and neck oncogenesis. International Journal of Molecular Sciences. 2019;20.
15. Kasiappan R, Kamarajan P, Kapila YL. Metabolomics in head and neck cancer: A summary of findings. In: Translational Systems Medicine and Oral Disease. Elsevier; 2019. p. 119–35.
16. Shin JM, Kamarajan P, Christopher Fenno J, Rickard AH, Kapila YL. Metabolomics of head and neck cancer: A mini-review. Frontiers in Physiology. 2016;7 NOV.

17. Rai V, Mukherjee R, Ghosh AK, Routray A, Chakraborty C. “Omics” in oral cancer: New approaches for biomarker discovery. Archives of Oral Biology. 2018;87:15–34.
18. Jelonek K, Pietrowska M, Widlak P. Systemic effects of ionizing radiation at the proteome and metabolome levels in the blood of cancer patients treated with radiotherapy: the influence of inflammation and radiation toxicity. International Journal of Radiation Biology. 2017;93:683–96.
19. Doyle L, Wang M. Overview of Extracellular Vesicles, Their Origin, Composition, Purpose, and Methods for Exosome Isolation and Analysis. Cells. 2019;8:727. doi:10.3390/cells8070727.
20. Zebrowska A, Skowronek A, Wojakowska A, Widlak P, Pietrowska M. Metabolome of exosomes: Focus on vesicles released by cancer cells and present in human body fluids. Int J Mol Sci. 2019;20.
21. Tian W, Liu S, Li B. Potential Role of Exosomes in Cancer Metastasis. 2019. doi:10.1155/2019/4649705.
22. Pang B, Zhu Y, Ni J, Thompson J, Malouf D, Bucci J, et al. Extracellular vesicles: The next generation of biomarkers for liquid biopsy-based prostate cancer diagnosis. Theranostics. 2020;10:2309–26.
23. Marrugo-Ramírez J, Mir M, Samitier J. Blood-Based Cancer Biomarkers in Liquid Biopsy: A Promising Non-Invasive Alternative to Tissue Biopsy. Int J Mol Sci. 2018;19:2877. doi:10.3390/ijms19102877.
24. Jelonek K, Widlak P, Pietrowska M. The Influence of Ionizing Radiation on Exosome Composition, Secretion and Intercellular Communication. Protein Pept Lett. 2016;23:656–63.
25. Jabbari N, Nawaz M, Rezaie J. Ionizing radiation increases the activity of exosomal secretory pathway in MCF-7 human breast cancer cells: A possible way to communicate resistance against radiotherapy. Int J Mol Sci. 2019;20.
26. Zorrilla SR, García AG, Carrión AB, Vila PG, Martín MS, Torreira MG, et al. Exosomes in head and neck cancer. Updating and revisiting. Journal of Enzyme Inhibition and Medicinal Chemistry. 2019;34:1641–51.
27. Xiao C, Song F, Zheng YL, Lv J, Wang QF, Xu N. Exosomes in Head and Neck Squamous Cell Carcinoma. Frontiers in Oncology. 2019;9.
28. Smolarz M, Pietrowska M, Matysiak N, Mielańczyk Ł, Widłak P. Proteome profiling of exosomes purified from a small amount of human serum: The problem of co-purified serum components. Proteomes. 2019;7.
29. Sullivan GM, Feinn R. Using Effect Size—or Why the P Value Is Not Enough . J Grad Med Educ. 2012;4:279–82. doi:10.4300/jgme-d-12-00156.1.
30. Cureton EE. RANK-BISERIAL CORRELATION. 1956.
31. Rosenthal, R. (1994). Parametric Measures of Effect Size. In H. Cooper, L. V. Hedges, & J. C. Valentine (Eds.), The Handbook of Research Synthesis (pp. 231-244). New York Russell Sage Foundation. - References - Scientific Research Publishing. https://www.scirp.org/(S(351jmbntvnsjt1aadkposzje))/reference/ReferencesPapers.aspx?ReferenceID=1985786. Accessed 13 Jul 2020.

32. Goenawan IH, Bryan K, Lynn DJ. DyNet: visualization and analysis of dynamic molecular interaction networks. doi:10.1093/bioinformatics/btw187.
33. Warburg O. On the Origin of Cancer Cells. 1956.
34. Lazar I, Clement E, Attane C, Muller C, Nieto L. Thematic review series: Exosomes and microvesicles: Lipids as key components of their biogenesis and functions: A new role for extracellular vesicles: How small vesicles can feed tumors' big appetite. Journal of Lipid Research. 2018;59:1793–804. doi:10.1194/jlr.R083725.
35. Record M, Carayon K, Poirot M, Silvente-Poirot S. Exosomes as new vesicular lipid transporters involved in cell–cell communication and various pathophysiologies. Biochim Biophys Acta - Mol Cell Biol Lipids. 2014;1841:108–20. doi:10.1016/j.bbalip.2013.10.004.
36. Kim EJ, Lee M, Kim DY, Kim K Il, Yi JY. Mechanisms of Energy Metabolism in Skeletal Muscle Mitochondria Following Radiation Exposure. Cells. 2019;8. doi:10.3390/cells8090950.
37. Gossai D, Lau-Cam CA. The effects of taurine, taurine homologs and hypotaurine on cell and membrane antioxidative system alterations caused by type 2 diabetes in rat erythrocytes. In: Advances in Experimental Medicine and Biology. Adv Exp Med Biol; 2009. p. 359–68. doi:10.1007/978-0-387-75681-3_37.
38. Jelonek K, Pietrowska M, Ros M, Zagdanski A, Suchwalko A, Polanska J, et al. Radiation-induced changes in serum lipidome of head and neck cancer patients. Int J Mol Sci. 2014;15:6609–24.
39. Jelonek K, Krzywon A, Jablonska P, Slominska EM, Smolenski RT, Polanska J, et al. Systemic Effects of Radiotherapy and Concurrent Chemo-Radiotherapy in Head and Neck Cancer Patients—Comparison of Serum Metabolome Profiles. Metabolites. 2020;10:60. doi:10.3390/metabo10020060.
40. Abramowicz A, Wojakowska A, Marczak L, Lysek-Gladysinska M, Smolarz M, Story MD, et al. Ionizing radiation affects the composition of the proteome of extracellular vesicles released by head-and-neck cancer cells in vitro. J Radiat Res. 2019;60.
41. Abramowicz A, Łabaj W, Mika J, Szołtysek K, Ślęzak-Prochazka I, Mielańczyk Ł, et al. MicroRNA Profile of Exosomes and Parental Cells is Differently Affected by Ionizing Radiation. Radiat Res. 2020.
42. Kumar Jella K, Rani S, O'Driscoll L, McClean B, Byrne HJ, Lyng FM. Exosomes Are Involved in Mediating Radiation Induced Bystander Signaling in Human Keratinocyte Cells. Radiat Res. 2014;181:138–45.

Tables

Table 1. Metabolites that differentiated cancer patients and healthy individuals

Metabolite name	Class	Mean abundance in cancer (samples A)	Mean abundance in control (samples C)	Significance of differences between control and cancer [RBCC effect size]
Serum metabolites				
		Upregulated in cancer		
Myristic acid	Fatty acids	3.90E-03	3.18E-03	**0.82**
Hypoxanthine	Purines	3.48E-04	1.46E-04	**0.76**
L-Glutamic acid	Amino acids	4.97E-03	2.34E-03	**0.70**
Xanthine	Purines	2.96E-05	2.01E-05	**0.66**
beta-Lactose	Saccharides	2.41E-05	9.82E-06	**0.64**
L-Serine	Amino acids	8.19E-03	6.07E-03	**0.60**
Oleic acid monoglyceride	Glycerolipids	2.41E-05	3.14E-05	**0.60**
O-Acetylserine	Amino acids	4.37E-03	3.60E-03	**0.58**
Eicosenoic acid	Fatty acids	3.61E-05	2.18E-05	**0.58**
Palmitoleic acid	Fatty acids	1.02E-03	3.12E-04	**0.56**
Oleamide	Fatty acids	6.71E-05	1.72E-05	**0.54**
L-Aspartic acid	Amino acids	2.02E-03	1.32E-03	**0.52**
		Downregulated in cancer		
Inosine	Purines	4.55E-05	4.28E-04	**-1.00**
Salicylic acid	Carboxylic acids	6.74E-06	8.44E-04	**-0.92**
Adenosine	Purines	1.27E-05	5.74E-05	**-0.89**
2-Ethylhexanoic acid	Fatty acids	1.14E-04	2.51E-04	**-0.74**
Gentisic acid	Carboxylic acids	6.36E-06	1.56E-05	**-0.64**
D-Threitol	Sugar alcohols	2.01E-04	2.88E-04	**-0.64**
Oxalic acid	Carboxylic acids	2.08E-02	2.47E-02	**-0.62**
Paraxanthine	Purines	1.94E-04	4.26E-04	**-0.62**
Serotonin	Amines	5.43E-05	1.06E-04	**-0.60**
D-Ribose	Saccharides	1.50E-04	1.51E-04	**-0.60**
N-acetyl-d-hexosamine	Amines	6.21E-05	1.69E-05	**-0.57**
Nonanoic acid	Fatty acids	2.23E-04	2.67E-04	**-0.56**
D-Xylonic acid	Sugar acids	3.07E-05	4.48E-05	**-0.56**
Phosphate	Inorganic acids	1.40E-02	1.64E-02	**-0.54**
L-Isoleucine	Amino acids	2.69E-03	3.30E-03	**-0.52**
Exosome metabolites				
		Upregulated in cancer		
1-Hexadecanol	Fatty alcohols	5.81E-05	3.12E-05	**0.52**
		Downregulated in cancer		
4-Hydroxybenzoic	Carboxylic acids	8.05E-07	2.61E-05	**-0.66**

acid				
Citric acid	Carboxylic acids	8.58E-06	3.22E-04	**-0.54**
Propylene glycol	Others	2.89E-05	1.96E-04	**-0.52**

Table 2. Metabolites that were affected by radiotherapy

Metabolite name	Class	Mean abundance pre-RT (samples A)	Mean abundance post-RT (samples B)	Significance of differences between pre-RT and post-RT [Cohen's d effect size]
Serum metabolites				
Upregulated by RT				
Hypotaurine	Others	6.48E-05	1.09E-04	**-1.16**
Glycerol-1-phosphate	Glycerolipids	1.03E-04	1.46E-04	**-1.06**
Oleamide	Fatty acids	6.71E-05	1.77E-04	**-0.81**
Serotonin	Amines	5.43E-05	6.71E-05	**-0.81**
Downregulated by RT				
1-Methylhistidine	Amino acids	1.13E-04	7.84E-05	**0.96**
Urea	Others	1.81E-04	4.76E-02	**0.96**
Quinic acid	Others	7.48E-05	5.60E-05	**0.87**
2-ketoglucose dimethylacetal	Hydroxy acids	1.68E-04	7.86E-05	**0.85**
4-Deoxyerythronic acid	Sugar acids	4.44E-05	2.77E-05	**0.85**
Galactosylglycerol	Glycerolipids	4.55E-05	1.69E-05	**0.85**
Gentisic acid	Carboxylic acids	6.36E-06	3.78E-06	**0.85**
D-Xylitol	Sugar alcohols	2.29E-04	1.49E-04	**0.82**

Figures

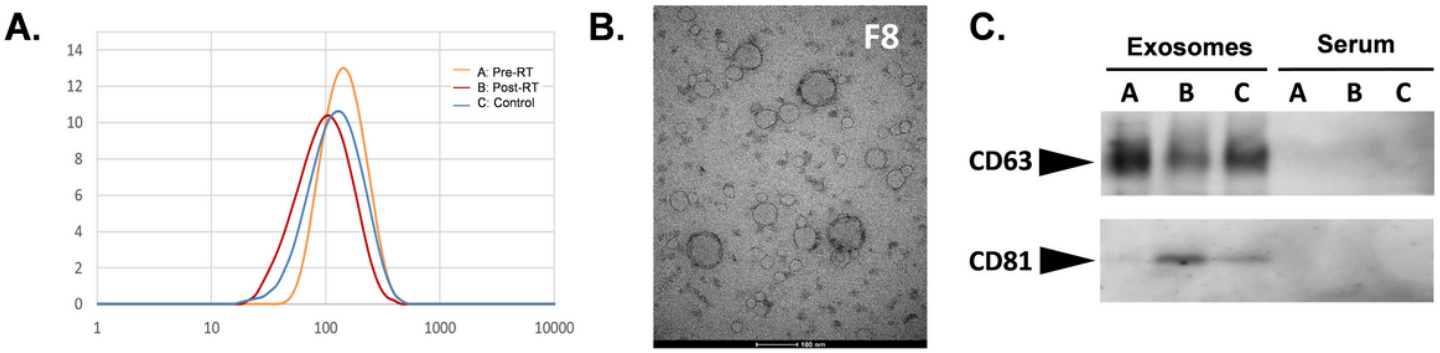

Figure 1

Characterization of serum-derived exosomes. Analysis of the size of vesicles in the SEC fraction #8 by the dynamic light scattering (A) and transmission electron microscopy (B). C - Western blot analysis of CD63 and CD81 in whole serum and serum-derived exosomes (fraction #8) for three groups of samples (A:pre-RT, B:post-RT, C:control).

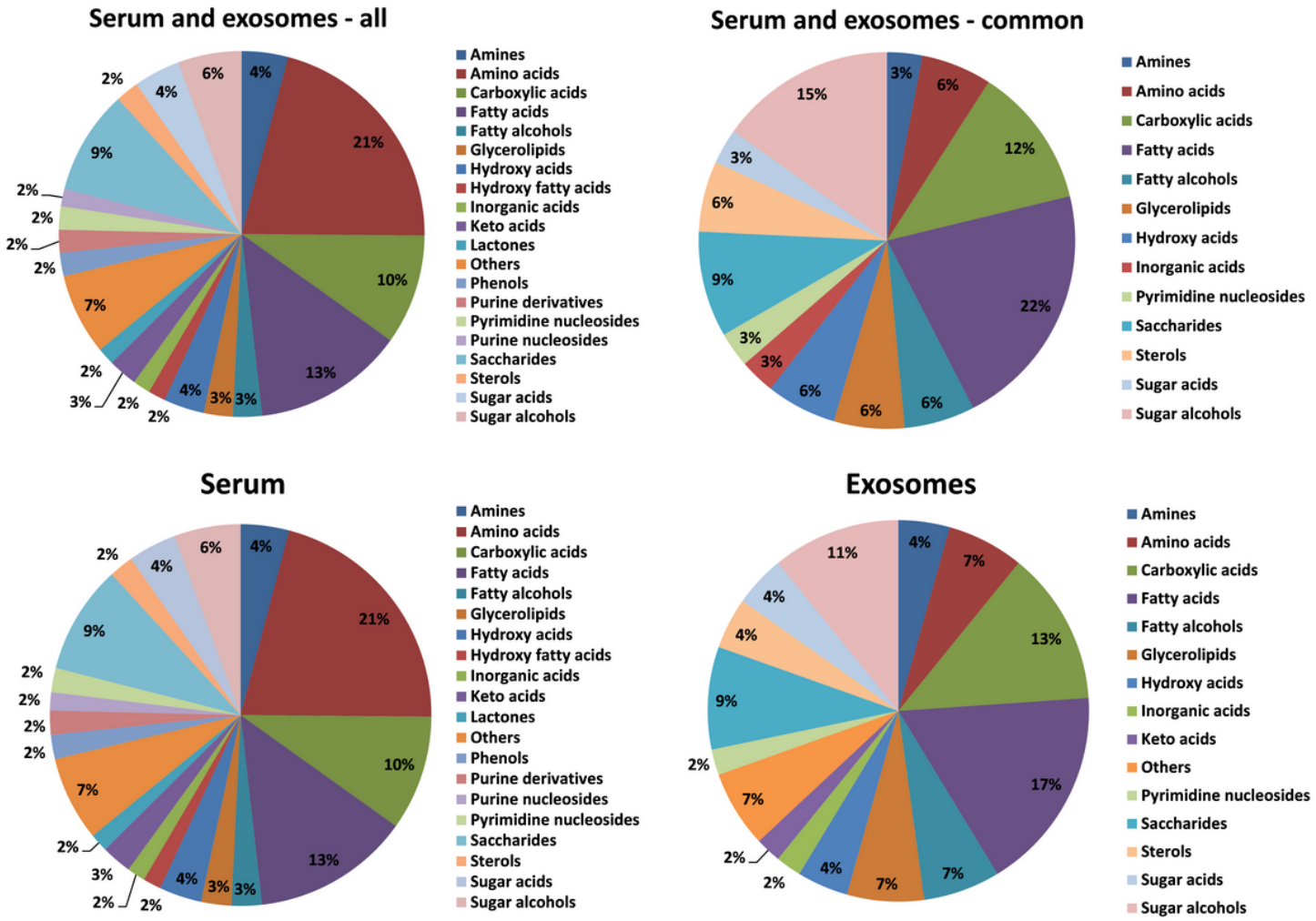

Figure 2

Relative Contribution of different classes of metabolites detected in serum and serum-derived exosomes.

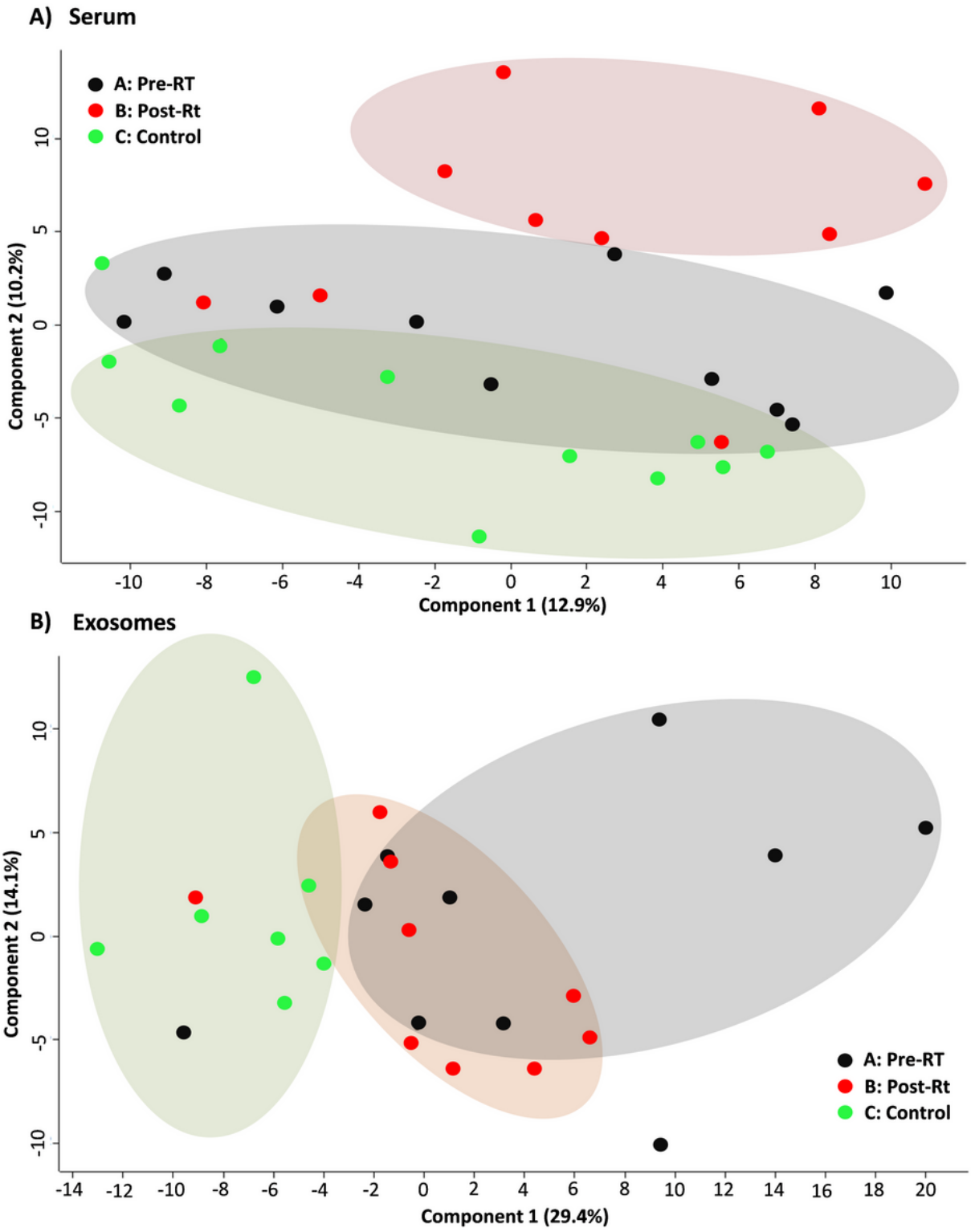

Figure 3

PCA score plots showing the clustering of cancer pre-RT samples A, cancer post-RT samples B, and control samples C. Showed are two first components responsible for 23.1% of the variability in the case of serum samples (A) and 43.5% of the variability in the case of exosome samples (B).

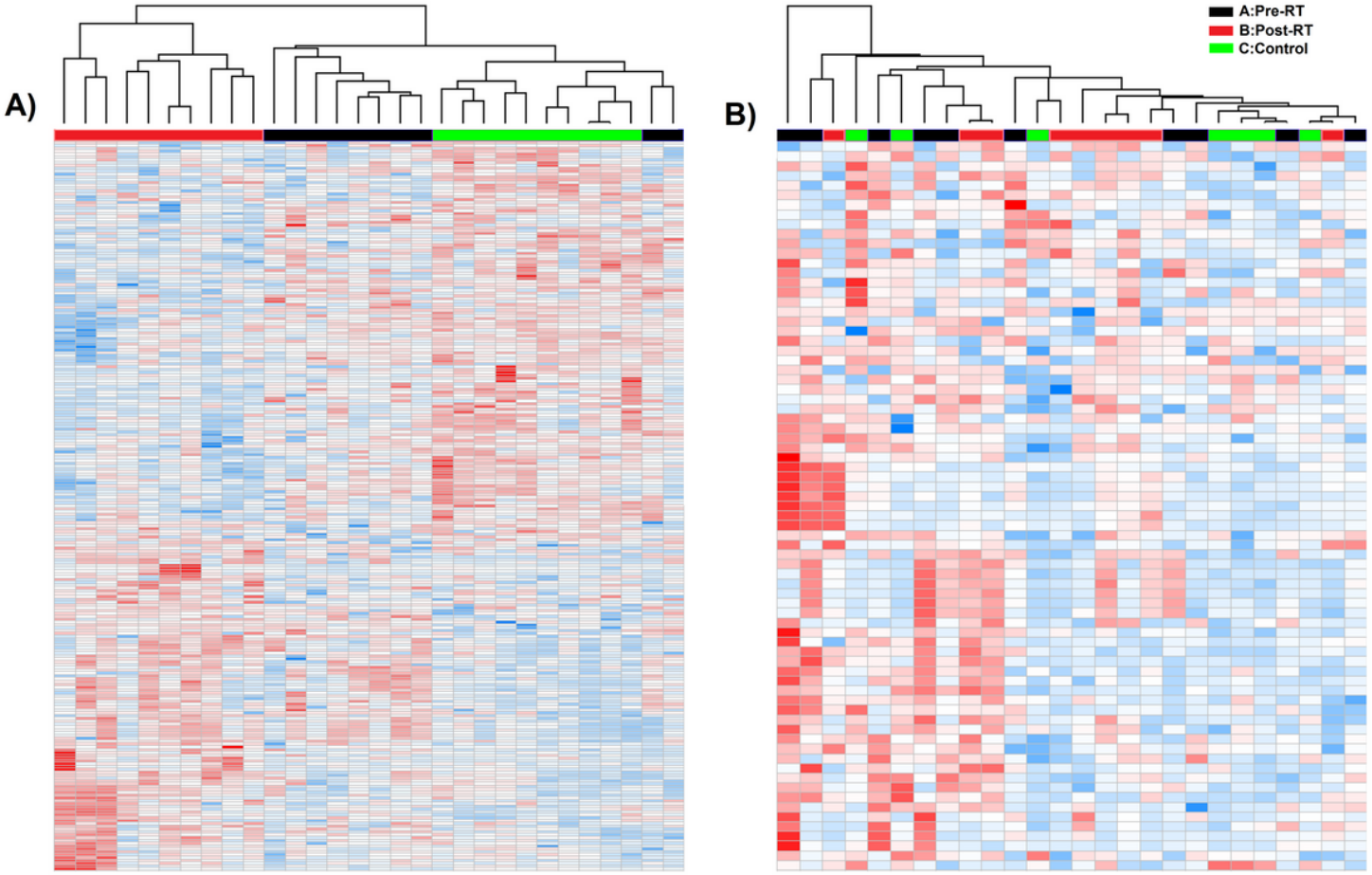

Figure 4

Hierarchical cluster analysis of cancer pre-RT samples A, cancer post-RT samples B, and control samples C. Showed are separate dendrograms for serum samples (A) and exosome samples (B)

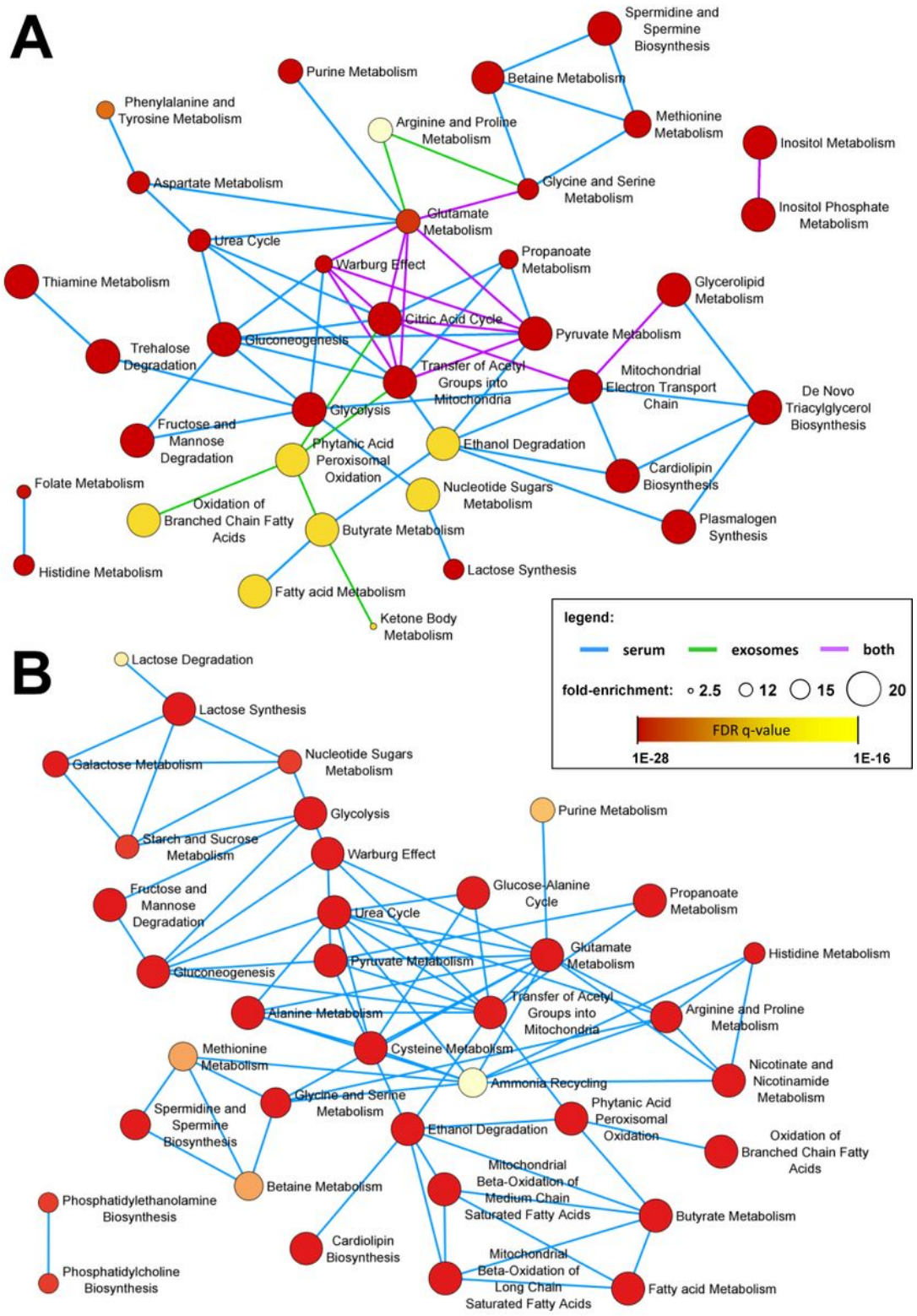

Figure 5

Metabolic pathways associated with specific subsets of compounds detected in the whole serum and serum-derived exosomes. Illustrated are over-represented pathways associated with metabolites differentiating between cancer and control samples (A) and between pre-RT and post-RT samples (B). The size of the network nodes corresponds to the pathway's fold-enrichment while the statistical significance of the over-representation is color-coded.

Supplementary Files

This is a list of supplementary files associated with this preprint. Click to download.

- SupplementaryTableS1.xlsx